JOURNAL OF APPLIED ELECTROCHEMISTRY **28** (1998) 151–160

Localized corrosion of 1024 mild steel in slightly alkaline bicarbonate solution with Cl^- ions

S. SIMARD, H. MÉNARD

Département de Chimie, Université de Sherbrooke, Sherbrooke, Québec, Canada J1K 2R1

L. BROSSARD

Institut de Recherches d'Hydro-Quebec (IREQ), Varennes, Québec, Canada J3X 1S1

Received 7 September 1996; revised 2 March 1997

The passive film breakdown of 1024 mild steel induced by the presence of 0.05 M chloride ions had been investigated in 0.075–0.75 M bicarbonate solutions at pH 8.9–9.7. A rotating disc electrode with a Kel-F holder was used in conjunction with a rotating ring-disc electrode. The resistance to localized attack is closely linked to the preanodization potential (E_{ox}) applied in the absence of Cl^- ions. For E_{ox} below about 0.2–0.3 V vs SCE, the resistance to localized attack provided by the passive film is independent of E_{ox}; above the breakdown potential, the localized attack is manifested by the formation of pits at the mild steel surface. The breakdown potential increases linearly with $NaHCO_3$ concentration and pH. Passive film breakdown for E_{ox} below about 0.2–0.3 V vs SCE most likely begins with a surface film dissolution prior to the penetration of the aggressive anions through the film. For E_{ox} above about 0.3 V vs SCE under the same conditions, no pitting is noticed and the potential associated with localized attack shifts considerably in the anodic direction due to interstitial (formation of crevices) corrosion at the mild steel/Kel-F interface.

Keywords: *corrosion*, *1024 mild steel*, *pitting*, *film breakdown*, *electro-oxidation*

1. Introduction

Many early papers deal with the breakdown of passive films on iron by aggressive anions in different buffers such as borate [1–8], acetate [4, 9], phosphate [10] or other media [8, 11–13]. It is well accepted that the thickness of the passive film for preanodized iron has a dominant effect for protection against pitting. The potential of preanodization is not reported as a significant parameter for the protection provided to iron by the passive film against localized attack by aggressive anions. However, studies have shown that for a critical preanodization charge, pitting occurs at the breakdown potential. The amount of oxide(s) generally ranges from 1 to a few mC cm^{-2}, which corresponds to a multilayer oxide film.

The study of protective properties of specific anodic films on mild steel in bicarbonate buffer has received little attention as far as localized attack is concerned. In a previous paper [14], it is pointed out that the nature of the passive film in deaerated bicarbonate solutions of pH 8.9 is potential-dependent. However, the film is very thin (i.e., in the range of one monolayer, a few tenths of mC cm^{-2}) in the presence of bicarbonate buffer compared to other buffers (6 mC cm^{-2} has been reported in borate buffer [5]).

As far as localized attack is concerned, the breakdown potential is well known to be an indicator of passive film stability in the presence of inhibitive and/or aggressive anions [15]. Little attention has been paid to passive film breakdown on iron in bicarbonate buffer [16]. From investigations of localized attack in selected buffers, the breakdown potential (E_b) can be linked to the concentration of aggressive anions by a linear relationship of $E_b = a + b \log[Cl^-]$ [16]. The measured values of a and b are related to several parameters such as the experimental technique, the solution pH, the nature and concentration of the buffer, temperature and surface preparation.

Compared to pure iron, the passivation and localized corrosion behaviour of alloys such as mild steel are generally related to many other factors, for example, the presence of metallic and/or nonmetallic inclusions [17]. The study of an alloy may give more scattered results for the breakdown potential compared to a pure metal or monocrystals. Such scattering of E_b values has lead some scientists to consider a stochastic approach [18] but results obtained by classical methods are still providing relevant information.

The present paper deals with the characterization of the localized attack of prepassivated 1024 mild steel in bicarbonate solutions after the addition of chloride ions as aggressive anions. Moreover, particular attention is paid to the protection provided by anodic films formed at different potentials. Since the passive film formed on 1024 mild steel in the presence

of $NaHCO_3$ (pH 8.9) is very thin [14] compared to that formed in the presence of other buffers for pure iron, it may be inferred that the protection against localized attack induced by the presence of Cl^- ions is different in $NaHCO_3$ compared to other buffers.

2. Experimental details

The experiments were carried out with a rotating disc electrode or a rotating ring-disc electrode to avoid mass transfer limitations. The disc electrode was made with a mild steel (1024) disc with the following chemical composition (% wt.): Fe 98.6, C 0.162, Mn 0.93, P 0.008, S 0.007, Si 0.20, Cu 0.008, Ni 0.005, Cr 0.037, V 0.004, Mo 0.018, Co 0.005, Sn 0.002, Al 0.037, Ti 0.005, Nb 0.003. A pure iron disc with an iron grade 'V.P.' from Materials Research Corporation (Orangebury, USA) was also used.

The disc electrodes had a surface area of 0.126 cm^2 and the metal rods were set in Kel-F holders. The rotating gold ring-steel disc electrode had a steel disc diameter of 5 mm while the gold ring had an inner diameter of 5.15 mm and an outer diameter of 7.2 mm (N = 0.4715 [19]). The auxiliary electrode was a platinized platinum grid separated from the main compartment by a Nafion® membrane. The reference electrode was a saturated calomel electrode (SCE) connected to the cell by a bridge and a Luggin capillary. All potentials further quoted in this investigation refer to this electrode. Since the presence of aqueous Fe(II) in the solution can influence the nature of the oxide film [20], the volume of the electrochemical cell used was 0.55 L or more; hence, the concentration of dissolved iron in the bulk of the solution may be neglected.

Aqueous solutions were prepared with BDHAssured® or Anachemia® analytical reactant grade chemicals using deionized water. The solutions were deaerated by high-purity nitrogen bubbling before and during the course of the experiments. The electrode surface was ground with 600, 3/0 emery paper and mechanically polished with 1.0 μm and 0.05 μm alumina suspensions before each immersion.

The measurements on the rotating disc electrode were performed with a PAR 273A potentiostat controlled by a computer, using M270 electrochemical software. The measurements with the rotating ring-disc electrode were taken with a Pine Instrument Company (Grove City, USA) bipotentiostat model AFRDE and the output signal was converted from analog to digital and recorded on an IBM-compatible computer using a customized software. The rotator of the electrodes was a Pine Instrument analytical rotator.

2.1. *Breakdown potential measurement methods*

The breakdown potentials were measured using two slightly different methods. (i) For a first set of experiments (Fig. 1(a) and (b)), the electrode surface was preanodized during 45 min (Q = 4.8 mC cm^{-2}) at a constant potential, E_{ox}, ranging from −0.4 to 0.8 V, in the absence of any Cl^- ions in the solution. Immediately after, the chloride ion solution was added and the potential was scanned in the anodic direction from −0.4 V for $E_{ox} \leq 0.2$ V (Fig. 1(a)) or from 0.25 V for $E_{ox} > 0.2$ V (Fig. 1(b)). The potential sweep rate (dE/dt) was 1 mV s^{-1} and the potential scan was stopped at the film breakdown potential. (ii) In this set of experiments (Fig. 1(c)), all the samples were preanodized at E_{ox} = 0.8 V during 45 min in the absence of chloride ions. After the film growth up to Q = 4.8 mC cm^{-2}, the potential was

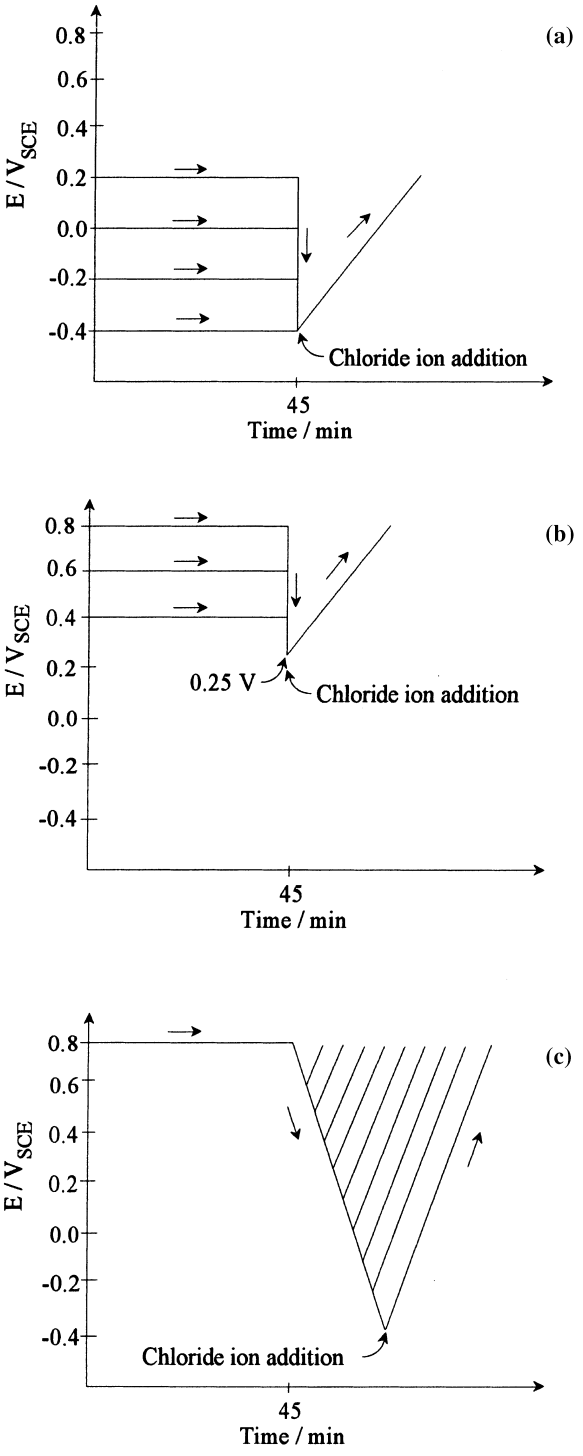

Fig. 1. Applied potential against time for the determination of the breakdown potentials.

swept at the rate of 1 mV s^{-1} from 0.8 V to a selected value ranging from −0.4 to 0.6 V. Immediately after, a chloride solution was injected into the cell and the potential sweep was reversed into the anodic direction. The potential scan (dE/dt = 1 mV s^{-1}) was stopped just after film breakdown.

2.2. *Induction time measurement methods*

The current versus time curves used to evaluate the induction times were recorded after a preanodization time of 45 min to give Q = 4.8 mC cm^{-2} at constant potential values, and a stock chloride solution was injected in the working solution immediately after preanodization. The potential was maintained at its initial value and the current versus time curves were recorded until film breakdown or for a maximum of 75 min in the absence of any film breakdown.

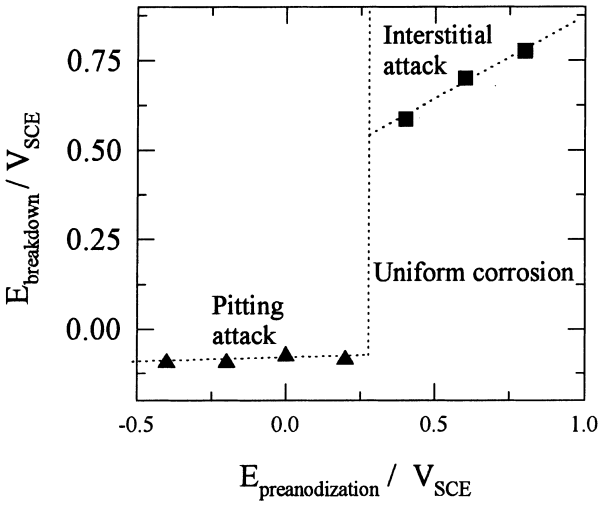

Fig. 2. Breakdown potential against preanodization potential. Solution: 0.2 M $NaHCO_3$, pH 8.9. Final concentration of Cl^- 0.05 M. ω = 1000 rpm. Applied potentials are given in Fig. 1(a) and (b). Preanodization time 45 min.

3. Results

3.1. *Breakdown potentials from potentiodynamic measurements*

Breakdown potential values (E_b) are given against E_{ox} in Fig. 2. A transition for E_{ox} close to about 0.2–0.3 V is noticed. For E_{ox} up to 0.2–0.3 V, the resistance of the film to the localized attack induced by the presence of chloride ions is practically independent of E_{ox}. It can also be observed from Table 1 that the film breakdown potential is similar for pure iron and mild steel. The localized attack is due to pitting (e.g., on Fig. 3(a), the electrode was preanodized at 0.0 V and pit formation is noticed).

For E_{ox} values larger than about 0.3 V, the breakdown potential considerably shifts in the anodic direction and increased anodization in E_{ox} entails that of E_b (Fig. 2); it is also observed that the localized attack takes the form of interstitial corrosion through the formation of crevices at the mild steel/Kel-F interface without any pitting (e.g., in Fig. 3(b), the electrode was preanodized at 0.8 V and interstitial corrosion was noticed). It is relevant to point out that the breakdown potential corresponding to the formation of crevices at the mild steel/Kel-F interface may vary largely under the same experimental conditions. Consequently, five breakdown potential measurements under the same experimental conditions were carried out and the minimum value of E_b for each set of experiments was considered.

A potentiodynamic trace in the cathodic direction of an electrode previously preanodized at 0.8 V during 3 h in the presence of 0.2 M $NaHCO_3$ at pH 8.9 shows a broad reduction current peak with its maximum being located at about −0.1 V (Fig. 4). This peak is ascribed to the reduction of a part of the oxide species formed during preanodization. Hence, to avoid further reduction of this protective film prior to its breakdown, the applied potential must be larger or close to 0 V at any moment during the measurements. The breakdown potentials were measured with such considerations.

3.2. *Induction times at constant potential*

The induction time required for the establishment of the film breakdown was measured for further characterization of the localized attack process. Typical current versus time curves for mild steel in the presence of chloride ions (0.05 M) are illustrated in Fig. 5, with constant applied potentials (E_{ox}) ranging from −0.4 to 0.6 V. The chloride ions were added to the solution after 45 min of preanodization and $E = E_{ox}$ before and after preanodization. For the recordings at −0.4 and −0.2 V, the oxidation current noticed is

Table 1. Breakdown potentials obtained using method i (Fig. 1(a))*

Preanodization potential, E_{ox} /V	*Iron* *−0.400 V*	*1024 Mild steel* *−0.400 V*	*−0.200 V*	*0.000 V*	*0.200 V*
E_b 1	−0.079	−0.085	−0.091	−0.085	−0.095
E_b 2	−0.089	−0.100	−0.089	−0.060	−0.092
E_b 3	−0.087	−0.101	−0.096	−0.067	−0.085
E_b 4	−0.085	−0.112	−0.096	−0.079	−0.095
E_b 5	−0.106	−0.080	−0.090	−0.093	−0.070
E_b $\bar{x}$	−0.089	−0.096	−0.096	−0.077	−0.087
	(σ_x = 0.009)	(σ_x = 0.012)	(σ_x = 0.003)	(σ_x = 0.012)	(σ_x = 0.09)

* Localized attack observed was by pitting in all cases.

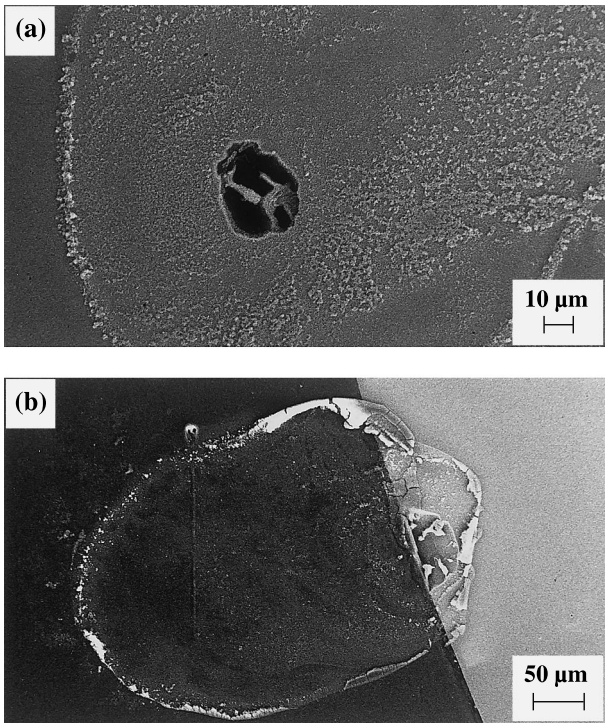

Fig. 3. SEM picture of 1024 mild steel electrode after localized attack. Solution: 0.2 M $NaHCO_3$, pH 8.9. Final concentration of Cl^- 0.05 M. $\omega = 1000$ rpm. (a) $E_{ox} = 0.0$ V; (b) $E_{ox} = 0.8$ V.

not negligible and very small current oscillations are observed for $E = -0.2$ V for a large enough polarization time; the current is most likely linked to metastable pitting and/or uniform dissolution of mild steel.

For potential values of −0.1, 0.0 and 0.1 V, which are close or above the breakdown potential, localized attack by pitting is quickly noticed. For $E = -0.1$ V, current oscillations are observed. A single current oscillation is possibly linked to film repair after the formation of a single pit. For $E \geq 0.2$ V, localized attack is not observed after up to 4500 s of polarization in the presence of chloride ions and the oxidation current is quite small.

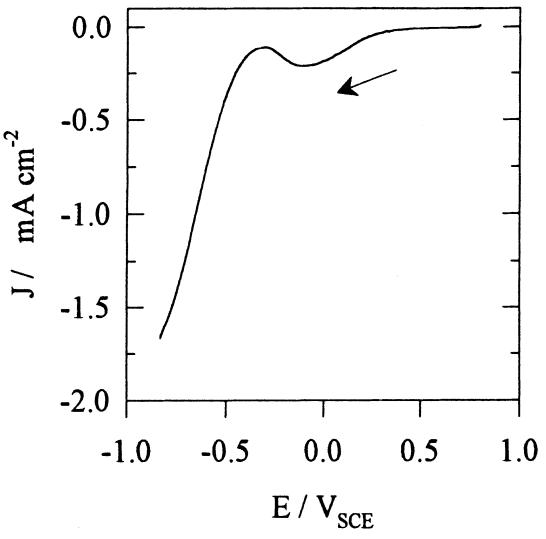

Fig. 4. Potentiodynamic trace for a potential sweep in the cathodic direction after 45 min preanodization at 0.8 V. Solution: 0.2 M $NaHCO_3$, pH 8.9. $\omega = 1000$ rpm. $dE/dt = 0.5$ V s^{-1}.

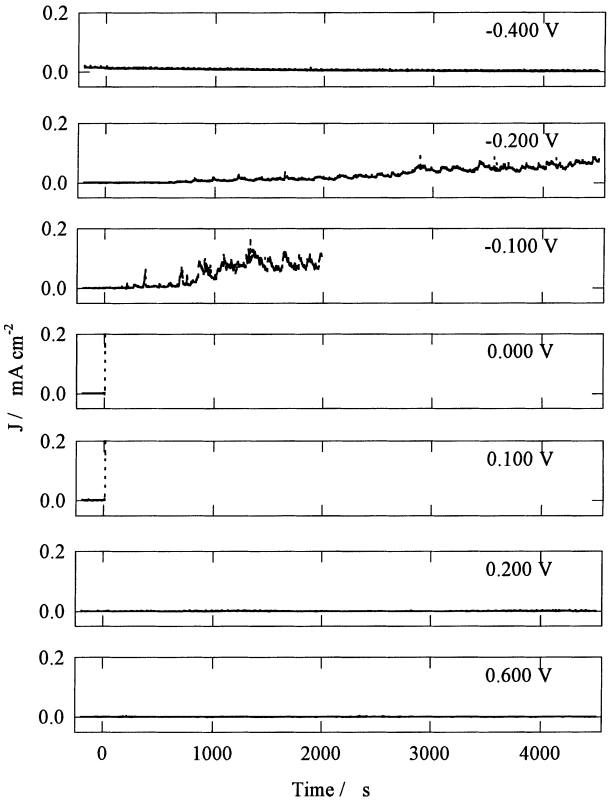

Fig. 5. Current against time curves at constant applied potential after preanodization during 2700 s at the same potential. Solution: 0.2 M $NaHCO_3$, pH 8.9. Final concentration of Cl^- = 0.05 M. $\omega = 1000$ rpm.

3.3. *Effect of pH*

The effect of pH on the pitting potential was investigated by the approach of Fig. 1(a) for a preanodization potential of −0.2 V. E_b is plotted against the solution pH on Fig. 6. A linear relationship of E_b against pH is noticed with a slope of about 0.125 V per pH unit. It is relevant to point out that the so-

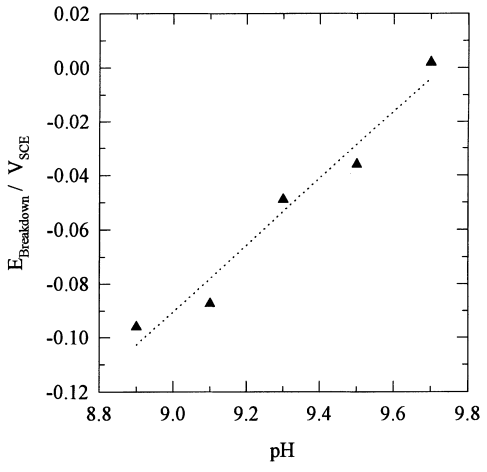

Fig. 6. Breakdown potentials measured at various solution pH. Solution: 0.2 M $NaHCO_3$. Final concentration of Cl^- 0.05 M. $\omega = 1000$ rpm.

Table 2. Breakdown potentials for 1024 mild steel obtained by method i† *(Fig. 1(c))*

Cathodic potential reversal, E_1 /V	*1*	*2*	*3*	*4*	*5*	E_b $(\bar{x})$ /V
−0.400	−0.045	−0.080	−0.100	−0.080	−0.058	−0.073 ($\sigma_x = 0.019$)
−0.200	−0.011	0.032	0.011	−0.017	−0.013	0.000 ($\sigma_x = 0.019$)
0.000	0.067	0.030	0.078	0.317	0.020	0.102 ($\sigma_x = 0.109$)
0.200	0.234	–	–	–	0.230	–
0.300	–	–	0.338	–	–	–
0.400	–	–	–	–	–	–
0.600	–	–	–	–	–	–

† For preanodization potential of 0.8 V.

lution composition is pH-dependent (Fig. 7); the concentration in HCO_3^- decreases but the concentration of both OH^- and CO_3^{2-} increases with pH.

3.4. *Effect of bicarbonate concentration*

Figure 8 illustrates the effect of the solution composition (pH 9) on the potentiodynamic behaviour of mild steel electrodes. A trace represents the potentiodynamic curve of mild steel in the presence of chloride ions without bicarbonate ions. Mild steel is passivated at low potentials up to about −0.3 V from which the localized attack is manifested by a significant current increase. The addition of 0.2 M $NaHCO_3$ to 0.05 M NaCl results in a large oxidation peak located at about −0.65 V. The oxidation peak is followed by a passive region extending over 0.4 V; close to $E = -0.1$ V, the sudden and considerable increase of the oxidation current is related to the film breakdown and formation of stable pits.

The effect of the bicarbonate concentration on the breakdown potential for preanodized samples under the experimental conditions of Fig. 1(a) is illustrated in Fig. 9. E_b shifts in the anodic direction as [$NaHCO_3$] is increased (Fig. 9 inset). It is also noticed that above 0.3 M $NaHCO_3$, the current oscillations tend to become larger and for [$NaHCO_3$] high enough (e.g., 0.75 M); the current oscillations become very large prior to the formation of stable pits. The current oscillations are associated with the successive local breakdown and repair of the protective film.

The current against time curves obtained for RRDE electrodes, with the mild steel oxidation potential maintained at −0.2 V, are characterized by two typical behaviours (Fig. 10). For Fig. 10(a), $E_{ring} = 0.4$ V, in order to oxidize soluble Fe(II) species generated during mild steel electrodissolution.

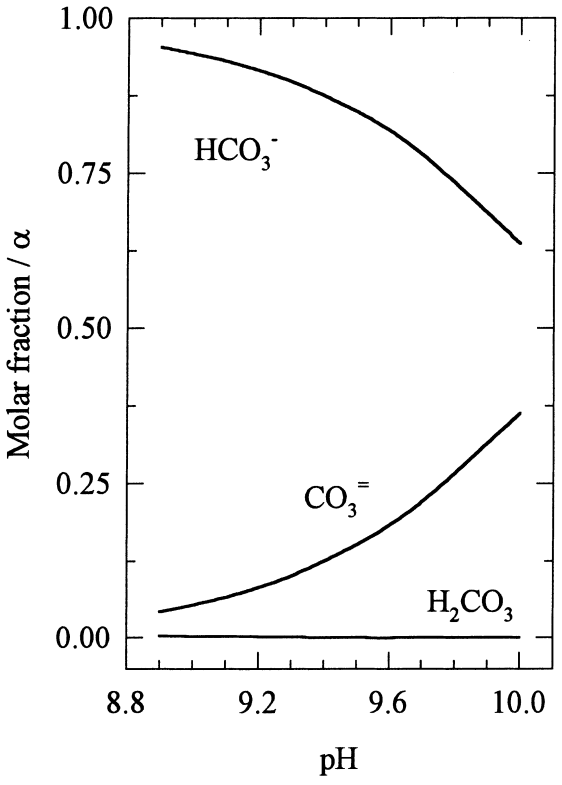

Fig. 7. Composition of a carbonate/bicarbonate buffer against pH (calculated from data of [31]).

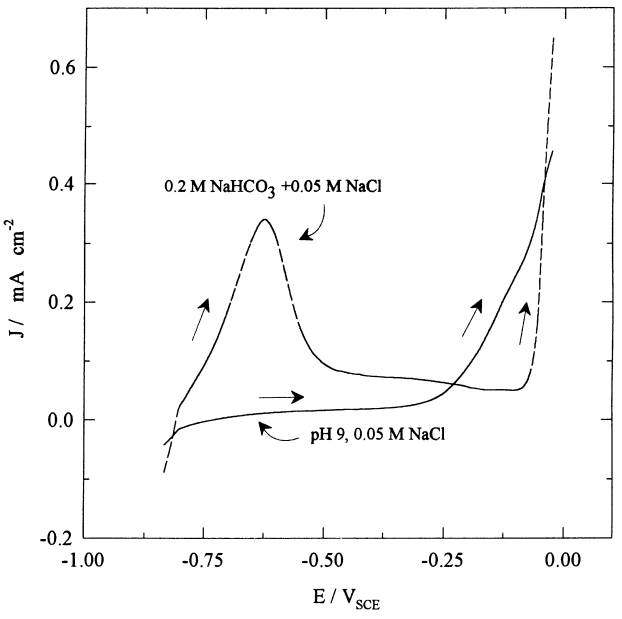

Fig. 8. Potentiodynamic curves for various concentrations of $NaHCO_3$ at pH 9. $dE/dt = 0.005\,Vs^{-1}$. $\omega = 1000$ rpm.

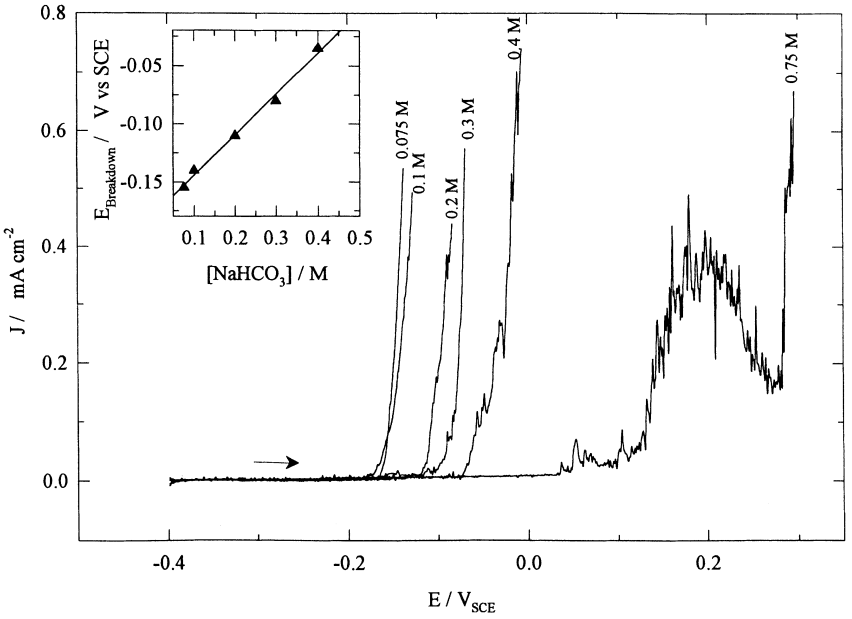

Fig. 9. Potentiodynamic traces for various bicarbonate concentrations in the presence of 0.05 M Cl^-. Solution: pH 8.9. Final concentration of Cl^- 0.05 M. $\omega = 1000$ rpm. Other experimental conditions are those of Fig. 1(a).

For Fig. 10(b), $E_{ring} = -0.55$ V in order to reduce the soluble Fe(III) species. From the i/t curves of Fig. 10(a), the oxidation current observed at the gold ring electrode is very small compared to the one noticed for the mild steel electrode, which indicates that the current linked to the dissolution of iron into soluble Fe(II) species electrogenerated at the disc electrode is negligible. A similar behaviour is observed in Fig. 10(b), that is, a quite small reduction current is detected at the ring electrode, which is attributed to an electrochemical reaction specific to the gold electrode because the same phenomenon is observed in the presence of a pure gold disc electrode.

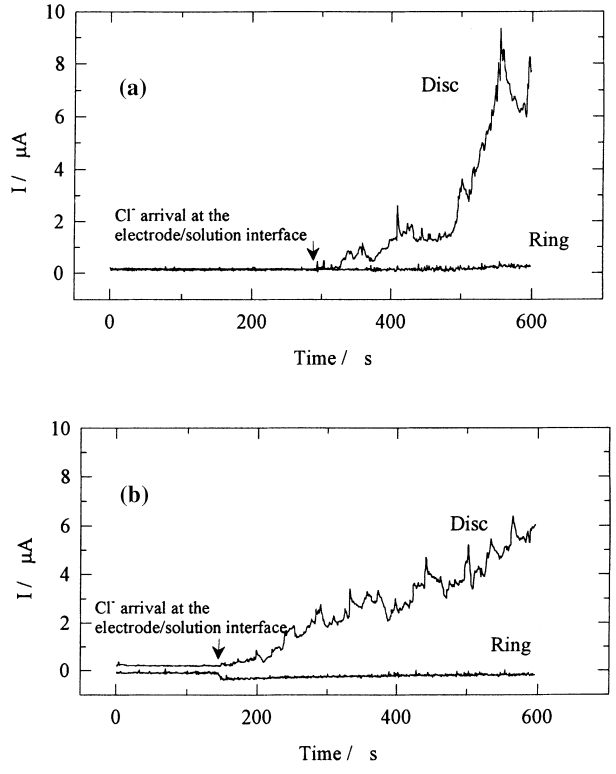

Fig. 10. i/t curves at ring-disc electrode. $E_{disc} = -0.2$ V, $E_{ring} = 0.4$ V. After preanodization during 2700 s. Solution: 0.2 M $NaHCO_3$, pH 8.9. Final concentration of $Cl^- = 0.05$ M. $\omega = 1000$ rpm. (a) $E_{ring} = 0.4$ V; (b) $E_{ring} = -0.55$ V.

A visual examination of the electrode surface after the curve recording of Fig. 10 showed the presence of a precipitate on the mild steel disc electrode surface. The electrochemical behaviour indicates that the precipitate is a poor inhibitor for oxidation of mild steel but no upright current increase is observed and the production of Fe(II) species in solution is avoided.

The understanding of the resistance of the film to breakdown is increased by i/t curves obtained after different oxidation times (Fig. 11). One sample was preanodized for 45 min (Fig. 11(a)) compared to 180 min for the other (Fig. 11(b)). Figure 11(a) shows that the current increases for both ring and disc electrodes is due to the fact that the chloride ions reach the surface of the electrodes. From Fig. 11(a) and (b), it is deduced that the longer the preanodization time (i.e., the larger the amount of the protective film formed during preanodization) the more protective the film against the localized attack induced by the presence of Cl^- ions.

In Fig. 12, a potentiodynamic curve is given for an RRDE disc, the potential of the disc being swept in the anodic direction until film breakdown; the potential at the gold-ring electrode is kept constant at 0.4 V to oxidize soluble species generated at the disc electrode. The curve recorded for the gold ring electrode is also illustrated. The oxidation current obtained at the ring electrode is correlated with the current at the mild steel disc electrode. Furthermore, in another set of experiments, the potential of the gold ring electrode was selected at −0.55 V in order to

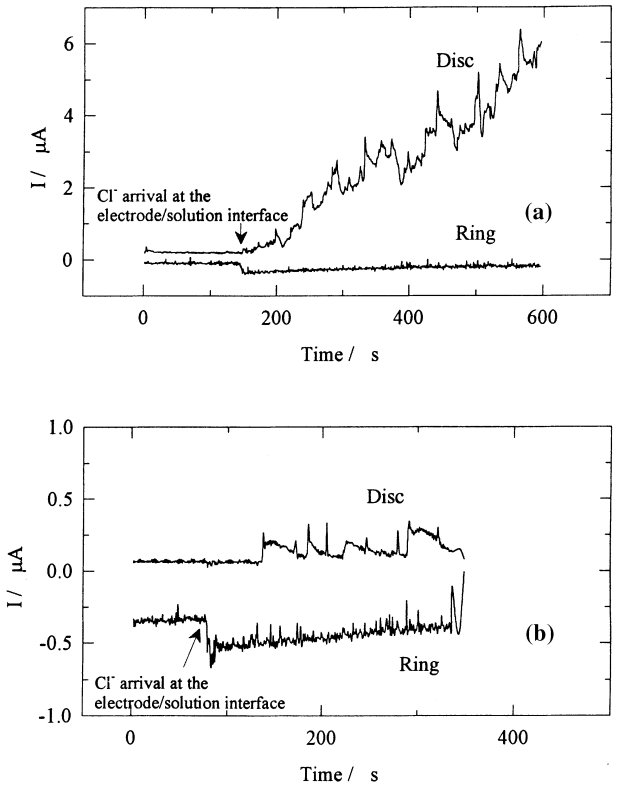

Fig. 11. i/t curves obtained for a ring-disc electrodes after preanodization of; (a) 45 min. (b) 180 min. $E_{disc} = -0.2$ V, $E_{ring} = 0.4$ V. Solution: 0.2 M $NaHCO_3$, pH 8.9. Final concentration of Cl^- 0.05 M, $\omega = 1000$ rpm.

reduce the Fe(III) soluble species possibly generated at the mild steel disc electrode during the potential scan under the experimental conditions of Fig. 12. The reduction current at the ring electrode was practically zero regardless of the oxidation current observed at the mild steel disc electrode even in the region of the film breakdown.

4. Discussion

The resistance of 1024 mild steel electrodes to the localized attack induced by the presence of Cl^- ions is significantly improved as E_{ox} is increased above a transition potential (i.e., 0.2–0.3 V), the preanodization being carried out in the presence of dissolved $NaHCO_3$ (Fig. 2). Moreover, the nature of the localized attack (i.e., formation of pits or crevices) is different for E_{ox} below or above the transition potential (Fig. 3) and a new solid oxide species is generated at the electrode surface as the preanodization potential is sufficiently anodic (0.2–0.3 V) (Fig. 4). Consequently, it may be deduced that the resistance of mild steel to localized attack is linked to the nature of oxide(s) formed during preanodization. Below the transition potential region, the breakdown potential is not dependent on the preanodization potential (Table 1). This observation is compatible with the works of Bardwell *et al.* [2] obtained on pure iron in borate buffer. The authors noted that the pitting potential was more dependent on the charge than the preanodization potential.

From previous works on iron and mild steel electrooxidation in slightly alkaline $NaHCO_3$ aqueous solutions [14], γ-Fe_2O_3 may form at potentials higher than 0.2–0.3 V compared to Fe_3O_4 and $Fe(OH)_2$ and/or $FeCO_3$ at low potentials [21]. The above seems to suggest that the resistance of 1024 mild steel electrode to pitting is considerably better when γ-Fe_2O_3 is present on the electrode surface. The protection offered by the presence of γ-Fe_2O_3 is consistent with the fact that the oxidation current remains negligible in 0.2 M $NaHCO_3$ + 0.05 M NaCl solution up to 4500 s of polarization (after preanodization) for a constant applied potential of 0.2 V or higher (Fig. 5).

In the pitting region, the breakdown potentials are similar for pure iron and mild steel after pre-

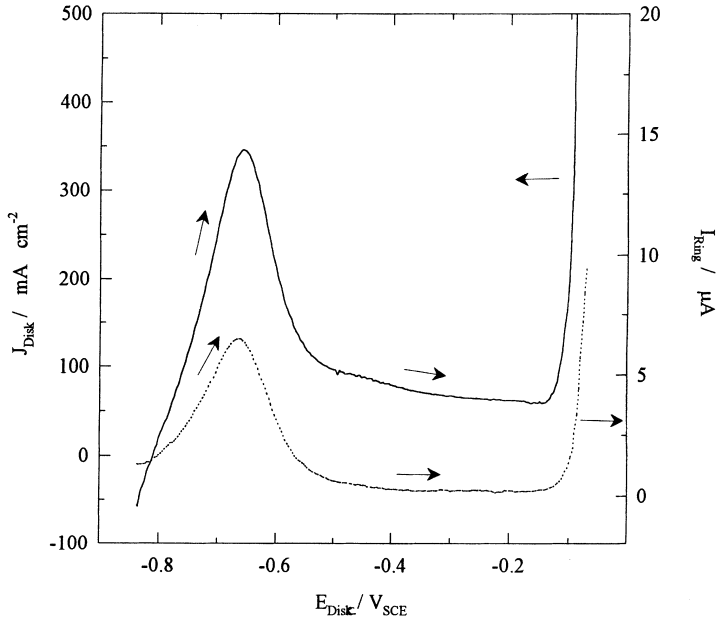

Fig. 12. Current at a gold ring electrode ($E = 0.4$ V) during a potential sweep of the mild steel disc electrode. Solution: 0.2 M $NaHCO_3$ and $Cl^- = 0.05$ M, pH 8.9. $\omega = 1000$ rpm. $(dE/dt) = 5$ mV s^{-1}.

anodization at −0.4 V (Table 1). This fact suggests that the presence of alloying elements and/or inclusions have practically no effect on the resistance of 1024 mild steel against localized attack for mild steel preanodized (E_{ox}) below 0.2 V.

As far as the effect of pH on pitting potential is concerned, the preanodization was carried out at low potentials and the formation of Fe_3O_4 with $Fe(OH)_2$ and/or $FeCO_3$ may be anticipated [22]. The relationship between E_b and the solution pH (Fig. 6) is explained by the fact that the solution composition plays a key role on the localized attack on 1024 mild steel. A pH increase has an inhibitive effect in this region of pitting potential which may be related to the contribution of both OH^- and CO_3^{2-} anions. It is not possible to determine their specific role in the corrosion process as inhibitors because the anions may be directly involved in the formation of a more stable film or they can act in a competitive adsorption with chloride ions, depending on the implied mechanism. An adsorption competition process was observed in NaOH media and considered to be involved in the first step of the passive film breakdown [11].

The presence of OH^- anions alone at pH 9 does not lead to steel electrodissolution in the range of active dissolution potential (~−0.65 V) but film breakdown is observed for $E \approx -0.25$ V in the presence of 0.05 M chloride ions (Fig. 8). Further, the addition of $NaHCO_3$ results in the formation of a strong oxidation peak current at low potentials which is related to the electrodissolution of steel in the form of Fe–HCO_3^-/CO_3^{2-} complexes. In the more anodic potential region, the mild steel is protected by a passive film up to its breakdown for $E \approx -0.1$ V. The comparison between the concentration in CO_3^{2-} and OH^- (i.e., at pH 9 for 0.2 M $NaHCO_3$; $[OH^-] \approx 10^{-5}$ M and $[CO_3^{2-}] \approx 10^{-2}$ M) suggests that the effect of CO_3^{2-} could be dominant compared to OH^-. Since the electrode was not previously preanodized and the potential sweep began at −0.835 V, the film formed on the surface during the potentiodynamic sweep could have similar characteristics as the film formed in the region below 0.2 V at constant applied potential. This is consistent with the fact that the localized attack arises by a pitting process. It indicates also that the growth of passive film is not prevented by the presence of chloride in solution and this behaviour is similar to the one reported earlier in borate buffer [23].

For films previously grown in solutions without any chloride ions, the linear relationship between [$NaHCO_3$] and E_b (Fig. 9) suggests that the presence of $NaHCO_3$ improves the resistance of the film against the localized attack induced by the presence of chloride ions. It is consistent with Fig. 8 where E_b increases as 0.2 M $NaHCO_3$ is added to a 0.05 M NaCl solution.

A theory concerning the breakdown of the anodic film reported by Sato [24] involves the effect of electrostriction due to the high electric field (10^6 V cm^{-1}) and surface tension. The surface tension stabilizes the passive film and it is deduced that the presence of adsorbed anions on the electrode surface lowers the surface tension and hence makes the film less stable. Considered purely from a thermodynamic point of view, this phenomenon is consistent with the loss of stability of passive film observed following the addition of aggressive anions, but it is clear that inhibitive anions also adsorb and decrease the surface tension. The consequences should be a decrease in stability, but it is well known that the experimentally observed effect is the opposite.

Among the vast literature on the corrosion of iron and its alloys, many papers discuss the elucidation of the breakdown mechanisms on iron. Three main mechanisms are usually discussed and reviewed in the literature [17, 25]. The penetration mechanism is related to the migration of aggressive anion or cation conductors [26] through the passive film with the assistance of the existing high electrical field (10^6–10^7 V cm^{-1}) across the film.

An adsorption mechanism is also suggested in the literature and experimental evidence finds this mechanism to be more effective for iron and nickel. The mechanism is induced by an adsorption of aggressive anions on the surface of the passive film. Afterwards, the aggressive anions complex with the cations from the oxide film and induce film dissolution. The latter phenomenon was reported in the literature and was characterized by the presence of halides leading to a thinning of the passive film [12, 27].

The current versus time curves recorded at constant potential (Fig. 5) show that the pitting phenomena is linked to the applied potential. For potential values lower than the film breakdown potential, the oxidation of the surface is linked to the formation of a poorly protective precipitate on the electrode surface. The current at the disc electrode starts to increase with time as Cl^- reaches the electrode/solution interface (Fig. 10). It is ascribed to the accumulation of Fe(II,III) solid species at the electrode surface due to the absence of a significant amount of soluble species detected at the RRDE. The damage caused by such attack is much less significant since no large corrosion current is involved if the oxidation is uniform over the entire surface. The corrosion process may be triggered by the presence of an anion permeable film. Moreover, in this region of potential, the competition between the breakdown and repair of the film can be expected in a similar range of frequency.

In the region of potential close to the breakdown potential (i.e., $E = -0.1$, 0 and 0.1 V), attack is quickly noticed (Fig. 5). This is a critical potential region where pitting is favoured.

The adsorption mechanism can be linked to the present study by i/t curves in Fig. 5. The behaviour observed, specifically for the measurements at −0.2 V, may be explained by such a mechanism. After the injection of chloride solution, a noticeable oxidation current is observed which increases at a practically constant rate. For a preanodization time of 45 min, the current increase starts as soon as the

chloride anions reach the electrode surface. Since the film under such experimental conditions is considered to be very thin (of the order of one monolayer [14]), it is clear that the fast formation of vacancy sites on the electrode surface allows the aggressive anions to attack the bare metal. The use of RRDE electrode shows that the oxidation product is a solid species generated at the surface (Fig. 10). It was found that no significant amount of soluble Fe(II) or Fe(III) species is generated by the metastable process. The metastable behaviour means also that the inhibitive performance of this solid is very poor. This solid may contain chloride ions as reported by some authors [8, 12, 28].

It can be summarized that the current measured below the breakdown potential is linked to the production of highly porous solid species on the electrode surface. Some work on the passive film breakdown on iron [29] reported that the pitting current may be split into two distinct terms. The first term is linked to pit nucleation and the second to pit growth. The low increasing rate of the current related to the localized attack in the latter region of potential may be related to the pit nucleation followed by pit repassivation.

For potentials higher than the transition region (0.2–0.3 V), the stability toward localized attack of the film is greatly improved, which is consistent with the results obtained by potentiodynamic measurements.

RRDE electrode measurements during iron disc oxidation (Fig. 12) suggest that the dissolution product generated after the film breakdown is related to the generation of soluble Fe(II) species. It is relevant to note an active dissolution at a potential around −0.1 V since it is observed that, with the use of a ring-disc electrode, the oxidation of soluble Fe(II) species produced at the disc electrode in the region of active dissolution (∼−0.7 V) starts at ∼−0.4 V at the gold ring electrode. It was demonstrated in the literature that the potential is not constant along the depth of the pit and in the bottom, the potential can be in an active dissolution region [30]. The electrogeneration of Fe(II) after pitting at −0.1 V strongly favours the existence of a potential gradient along the depth of the pits.

The preanodization time is an important parameter regarding the breakdown resistance of the passive film as well. RRDE experiments reported in Fig. 11 show a significant incubation time for samples preanodized for 180 min. This time delay may be attributed to the time of the passive film dissolution by the action of the aggressive anions. If one considers the dissolution of a passive film related to a catalytic effect from aggressive anions, it may be deduced that oxide film is gradually dissolved and the time necessary to sufficiently thin the film corresponds to the incubation time prior to the film breakdown. Some authors suggest that the passive film thickness may be reduced to a critical value where the pitting can occur [12]. However, since the charge associated with the film reduction is very small [14], it is deduced that the ring electrode is not sensitive enough to detect the presence of ions generated during the film thinning.

The dependence of the incubation time on the preanodization time observed led us to consider a two-step mechanism. At low potentials, beginning by an adsorption mechanism, the aggressive anions promote the passive film dissolution and the creation of spots with bare metal is anticipated.

For the passive film formed at around 0.3 V or at higher potentials, its dissolution rate due to the presence of aggressive anions is practically not affected. In this case, the formation of bare metal spots is avoided and no pit nucleation is observed.

Moreover, for potentiodynamic measurements, an increase in the electrical field across the film must be expected. Hence, the breakdown should occur but no pit nucleation is observed. In this case, for this type of passive film, the penetration mechanism is not effective. This fact may be attributed to a compact form of film where the migration of anion or cation vacancy is prohibited or the breakdown mechanism must be an inclusive device of the adsorption and penetration mechanisms.

The third principal breakdown mechanism discussed in the literature is the film breaking mechanism [17]. This mechanism involves chemical changes or stress establishment within the film caused by a step of potential. Obviously, thin films like those observed in the present paper may be subject to such disturbances. A step of potential from the region over 0.2 V to a lower value will affect the passive film by a possible reduction of some oxide species.

In the future, efforts will be devoted to the spectroscopic *in situ* identification of the surface oxide films obtained under the experimental conditions of the present study to clarify the nature of the passive films formed at the electrode surface.

5. Conclusions

The presence of $NaHCO_3$ in solution has an inhibitive effect on the localized attack induced by the presence of chloride anions. The passive film, which is particularly thin in the media under consideration, shows two different behaviours toward the localized attack induced by the presence of Cl^- ions depending on the preanodization potential. Below 0.3 V, the breakdown of the film is practically constant with the preanodization potential. In this region of potential, a raise in the bicarbonate concentration or pH, increases the breakdown potential. Over 0.3 V, the film becomes much more stable and loses its sensitivity to pitting attack.

The breakdown mechanism below 0.2–0.3 V is suggested to be a multistage mechanism. The mechanism could begin by a thinning of the passive film due to a catalytic dissolution and followed by the aggressive anions reaching the metal surface. At this time, a severe localized attack occurs.

The product of oxidation below the pitting potential is a precipitate while over this pitting poten-

tial, soluble species of Fe(II) constitute the major part of the oxidation current.

Acknowledgements

The authors acknowledge the financial support of Hydro-Québec (IREQ), the Natural Sciences and Engineering Research Council of Canada (NSERCC) and the Fonds pour la Formation des Chercheurs et l'Aide à la Recherche (FCAR-Québec). Special thanks to Yves Bergeron for his helpful work in our laboratory.

References

[1] J. A. Bardwell, B. MacDougall and M. J. Graham. *J. Electrochem. Soc.* **135** (1988) 413.
[2] J. A. Bardwell and B. MacDougall. *ibid.* **135** (1988) 2157.
[3] J. A. Bardwell, B. MacDougall and G.I. Sproule. *ibid.* **136** (1989) 1331.
[4] J. A. Bardwell, J. W. Fraser, B. MacDougall and M. J. Graham. *ibid.* **139** (1992) 366.
[5] T. E. Pou, O. J. Murphy, V. Young and J. O'M. Bockris. *ibid.* **131** (1984) 1243.
[6] J. A. Bardwell and B. MacDougall. *Electrochem. Acta* **34** (1989) 229.
[7] C. L. McBee and J. Kruger, *in* 'Localized Corrosion', NACE-3, (edited by R.W. Staehle, B. F. Brown, J. Kruger and A. Agrawal), NACE. Houston. TX (1974), p. 252.
[8] K. E. Heusler and L. Fischer. *Workst. Corros.* **27** (1976) 551.
[9] J. A. Bardwell, B. MacDougall and M. J. Graham. *Corros. Sci.* **32** (1991) 139.
[10] M. Cohen, *Corrosion* **32** (1976) 461.
[11] H. E. H. Bird, B. R. Pearson and P. A. Brook, *Corros. Sci.* **28** (1988) 81.
[12] K. Ogura and M. Kaneko, *ibid.* **23** (1983) 1229.
[13] S. Juanto, J. O. Zerbino, M. I. Miguez, J. R. Vilche and A. J. Arvia. *Electrochim. Acta* **32** (1987) 1743.
[14] S. Simard, M. Drogowska, L. Brossard and H. Ménard. *J. Appl. Electrochem.*, **27** (1997) 317.
[15] N. Sato and G. Okamoto, *in* 'Comprehensive Treatise of Electrochemistry', Vol. 4 (edited by J. O'M. Bockris, B. E. Conway, E. Yeager and R. E. White), Plenum Press., NY (1981), p. 193.
[16] M. Ergun and A. Y. Turan. *Corros. Sci.* **32** (1991) 1137.
[17] H-H. Strehblow, *in* 'Corrosion Mechanism in Theory and Practice', (edited by P. Marcus and J. Oudar), Marcel Dekker, NY (1995), p. 201.
[18] C. Gabrielli, F. Huet, M. Keddam and R. Oltra, *in* 'Advances in Localized Corrosion'. (edited by H. S. Isaac, U. Bertocci, and J. Kruger), NACE, Houston, TX (1987), p. 93.
[19] W. J. Albery and M. L. Hitchman, 'Ring-Disk Electrodes', Clarendon Press, Oxford (1971).
[20] M. E. Bett, K. M. Parkin and M. J. Graham, *J. Electrochem. Soc.* **133** (1986) 2032.
[21] L. J. Simpson and C. A. Melendres. *ibid.* **143** (1996) 2146.
[22] E. Deltombe and M. Pourbaix, *in* 'Comportement électrochimique du fer en solution carbonique, diagrammes d'équilibre tension-pH du système Fe–CO_2–H_2O, *à* 25 °C'. Rapport technique 8. CEBELCOR (1954).
[23] M. J. Graham, J. A. Bardwell, R. Goetz, D. F. Mitchell and B. MacDougall. *Corros. Sci.* **31** (1990) 139.
[24] N. Sato, *Electrochim. Acta* **16** (1971) 1683.
[25] H.-H. Strehblow. *Workst. Corros.* **35** (1984) 437.
[26] D. D. Macdonald. *J. Electrochem. Soc.* **139** (1992) 3434.
[27] W. Khalil, S. Haupt and H.-H. Strehblow. *Workst. Corros.* **36** (1988) 16.
[28] S. Kesavan, T. A. Mozhi and B. E. Wilde, *Corrosion* **45** (1989) 213.
[29] R. Nishimura, M. Araki and K. Kudo. *ibid.* **40** (1984) 465.
[30] H. W. Pickering and R. P. Frankenthal. *J. Electrochem. Soc.* **119** (1972) 1297.
[31] H. Freizer and Q. Fernando, *in* 'Ionic Equilibria in Analytic Chemistry', J. Wiley & Sons, New York. NY (1963).